Appl. Phys. B 82, 141–148 (2006)
DOI: 10.1007/s00340-005-2050-8

Applied Physics B
Lasers and Optics

N. CAO[1,✉]
T. FUKUCHI[2]
T. FUJII[2]
R.L. COLLINS[3]
S. LI[3]
Z. WANG[1]
Z. CHEN[1]

Error analysis for NO_2 DIAL measurement in the troposphere

[1] Electrical Department, Nanjing University of Infromation Science and Technology, 114 Pancheng street, Pukou, Nanjing city 210044 P.R. China
[2] Central Research Institute of Electric Power Industry, Electrical Physics Department, Komae Research Laboratory, 2-11-1 Iwado-kita, Komae-shi, Tokyo 201-8511, Japan
[3] Geophysical Institute, University of Alaska Fairbanks, 903 Koyukuk Drive, Fairbanks, AK 99775-7320, USA

Received: 28 March 2005/Final version: 17 September 2005
Published online: 30 November 2005 •

ABSTRACT NO_2 concentration profiles, which are important in studies of atmospheric chemistry and urban pollution, were measured by a differential absorption lidar (DIAL) based on a pair of Nd:YAG pumped dye lasers. In the experiments, 448.1 nm and 446.8 nm were used for "on" and "off" wavelengths, respectively. NO_2 concentration profiles of 0–40 ppb were obtained for altitudes between 900 and 2250 m with a 150 m range resolution. Null error, which was estimated by deviation of the null profile from zero, was < 2 ppb. The statistical error, systematic error from aerosols, and error due to uncertainty of absorption cross section were < 3.35 ppb, < 4.44 ppb and < 1 ppb, respectively. The total error was about 6.0 ppb. The estimation of aerosol backscatter and extinction error in NO_2 measurement due to inhomogeneous aerosol distribution is treated in detail.

PACS 42.68 Wt; 42.68 Kh; 42.68J

1 Introduction

Nitrogen dioxide (NO_2) is a typical atmospheric pollutant, the emission of which gives rise to serious problems for human health and the environment. In addition to its direct toxicity, NO_2 causes acidification of water, plays an important role in the formation of photochemical smog, and is active in atmospheric chemical reactions [1]. Monitoring of NO_2 is therefore of considerable interest and importance. DIAL (differential absorption lidar) systems have been used in measurement of NO_2 owing to their convenience in obtaining vertical concentration profiles. However, in the past, this method has been applied mostly for localized, relatively high concentrations, such as smokestack exhaust and industrial plant emission, where the NO_2 concentration is of the order of 60 ppb [2]. On the contrary , NO_2 concentration in the ambient atmosphere is substantially low. Consequently, vertical measurement in ambient air with inhomogeneous aerosol distribution is difficult.

There have been few reports on the effects of aerosols on NO_2 concentration profile measurement. Although some methods to estimate aerosol error for O_3 measurement have been proposed [3], they are all based on an assumed wavelength dependence of the aerosol backscatter and extinction coefficients, and based on an assumed aerosol scattering ratio profile with altitude [4, 5]. However, the validity of the assumptions is questionable because the aerosol conditions, especially the aerosol vertical profile, under investigation may be very different form those associated with the assumptions. In this paper, aerosol properties have been calculated from observed data only by the assumption of the wavelength dependence of the aerosol backscatter and extinction coefficients. In other words, aside from this assumption of the aerosol backscatter wavelength dependence, the aerosol error is estimated directly from actual experiment data.

In DIAL measurements, interference by other gases in the same wavelength region, effects due to differential aerosol backscatter and extinction, and effects due to differential Rayleigh backscatter and extinction should be considered. In the case of NO_2 measurement, while the separation between "on" and "off" wavelengths (448.1 nm and 446.8 nm) is small, interference due to differential aerosol backscatter may be significant, especially in regions of inhomogeneous aerosol distribution. In other words, gradients in aerosol backscatter due to aerosol layers may cause significant errors in DIAL measurement. The effects of Rayleigh backscatter and extinction can be calculated, since the wavelength dependence of Rayleigh scattering is well known. Interference by other gases can be neglected because their absorption cross-sections are much smaller than that of NO_2 in the wavelength region near 450 nm. In addition, the error due to uncertainty of absorption cross -section, systematic error due to beam misalignment, and statistical error are considered.

2 Experimental system

We have developed a DIAL system to monitor vertical concentration profiles of atmospheric trace substances (O_3, SO_2, NO_2, Hg) in the lower troposphere. The DIAL system incorporates two tunable dye lasers pumped by two Nd:YAG-lasers and a 50 cm diameter Newtonian telescope. The Nd:YAG lasers operate at a repetition rate of 10 Hz, and each dye lasers can emit two wavelengths (λ_a, λ_b) on alternate pulses, tunable within the oscillation range of the dye. The relative timing Δt of the two pump lasers is variable and can be set by a delay generator so that the transmitter can emit

✉ Fax: 86-025-58731195, E-mail: nwcao@yahoo.com.cn

a sequence of four wavelengths consisting of two wavelength pairs separated by Δt.

In NO_2 DIAL measurement, one dye laser with Coumarin 445 dye pumped by the third harmonic of an Nd:YAG laser (355 nm) was used. The wavelength 448.1 nm and 446.8 nm were used for "on" and "off" wavelengths, respectively. The case $\lambda_a = 446.8$ nm, $\lambda_b = 448.1$ nm is defined as DIAL1, the case λ_a=448.1 nm, $\lambda_b = 446.8$ nm is defined as DIAL2, and the case $\lambda_a = 446.8$ nm, $\lambda_b = 446.8$ nm is defined as null. A series of two DIAL measurements and one null measurement were performed over a period of 24 hours, with the sequence of DIAL and null measurements repeated every 2 hours. The laser beams used for 448.1 nm and 446.8 nm were swapped in two DIAL measurements. Each measurement consisted of a sequence of five profiles, each with 2 minute integration time. The total number of laser shots for the five profiles was 3000 shots for each wavelength. In DIAL1, DIAL2, and null measurement, the pulse energy was about 18 mJ, 15 mJ,and 12 mJ, respectively. The energy decreased gradually, owing to the lifetime of Coumarin 445, so the dye solution was replaced for each series of measurements. Laser beams were transmitted vertically after being expanded by a beam expander to about 2.5 cm diameter. The telescope focused backscattered light onto a field stop whose field of view is 3 mrad. The backscatter light is collimated and converted to an electrical signal by a photomultiplier tube (PMT, Hamamatsu R3896). We put an interference filter at the center wavelength 447.7 nm and bandwidth 4.6 nm, in front of the PMT. The filter transmission is 0.70 at 448.1 nm and 0.67 at 446.8 nm, and the PMT quantum efficiency is 0.23. In order to reduce the light intensity an ND filter with 5% transmission was also used. The telescope reflectivity (including both primary and secondary mirrors) is 0.84. The total optical efficiency of the receiver, obtained from the telescope reflectivity, PMT quantum efficiency and filter transmission, is 0.14 at 448.1 nm and 446.8 nm. The PMT is gated by a high voltage gate pulse of risetime 3.3 μs, falltime 3.5 μs, duration 250 μs. PMT signals are digitized by a 12 bit, 20 MHz digitizer (GaGe CS1012) corresponding to a range resolution of 7.5 m.

3 Experimental result

The range-resolved NO_2 concentration profile was obtained by

$$N(z) = -\frac{1}{2\Delta\sigma}\frac{\mathrm{d}}{\mathrm{d}z}\left[\ln\frac{P_{\lambda_{\mathrm{on}}}(z)}{P_{\lambda_{\mathrm{off}}}(z)}\right], \quad (1)$$

where $\Delta\sigma$ is the differential absorption cross section, and $p_{\lambda_{\mathrm{on}}}(z)$ and $p_{\lambda_{\mathrm{off}}}(z)$ are the return signals at the "on" and "off" wavelengths, respectively. The absorption cross section of NO_2 was taken to be $7.11 \times 10^{-23}\,\mathrm{m}^2$ at 448.1 nm and $4.19 \times 10^{-23}\,\mathrm{m}^2$ at 446.8 nm [6], so $\Delta\sigma = 2.9 \times 10^{-23}\,\mathrm{m}^2$. The obtained return signals were processed as follows: (1) the background level, which was obtained from the PMT signal before the laser shots, was subtracted, (2) all signals were averaged over 20 time bins corresponding to a range resolution of $\Delta R = 150$ m, and (3) the concentration was calculated by (1).

The NO_2 concentration profiles for 900–2250 m altitude obtained from 21:50 to 22:20 on December 20, 1999, and from 1:30 to 2:00 on December 21, 1999, are shown in Figs. 1 and 2. Judging from the waveforms of the range-corrected signals which are averaged for 3000 laser shots (10 minutes integration time), Fig. 1 can be said to represent a case of inhomogeneous atmosphere, whereas Fig. 2 represents a case of clear atmosphere. In Fig. 1, we can see that the highest NO_2 concentration is obtained at an altitude of 1200 m, which may be due to the passage of an air mass including high concentrations of NO_2 and aerosols cross the measurement region of the lidar system.

In Figs. 1 and 2, the symbols and error bars represent the mean value and standard deviation of the sequence of five measurements. In Fig. 2, the null profile is nearly symmetric about 0 ppb, with an average value of 1.8 ppb for this height interval. On the contrary, the DIAL value are > 20 ppb

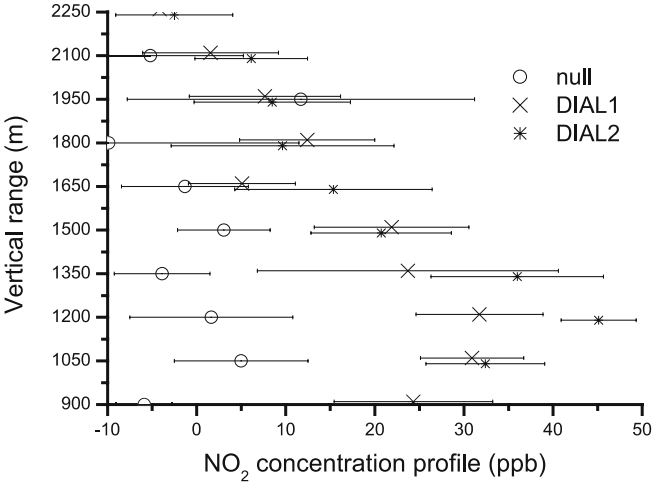

FIGURE 1 NO_2 concentration profiles obtained from 21:50 to 22:20 on Dec.20, 1999, in the case of inhomogeneous atmosphere: DIAL1 ($\lambda_a = 446.8$ nm, $\lambda_b = 448.1$ nm), DIAL2 ($\lambda_a = 448.1$ nm, $\lambda_b = 446.8$ nm), and null ($\lambda_a = 446.8$ nm, $\lambda_b = 446.8$ nm) are shown. The symbols represent the average value of NO_2 concentration and the error bars represent the standard deviation for the five profiles

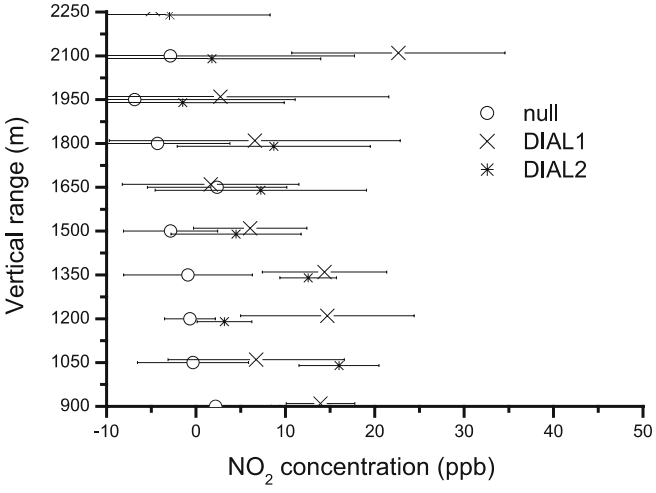

FIGURE 2 NO_2 concentration profiles obtained from 1:30 to 2:00 on Dec.21, 1999, in the case of clear atmosphere: DIAL1 ($\lambda_a = 446.8$ nm, $\lambda_b = 448.1$ nm), DIAL2 ($\lambda_a = 448.1$ nm, $\lambda_b = 446.8$ nm), and null ($\lambda_a = 446.8$ nm, $\lambda_b = 446.8$ nm) are shown. The symbols represent the average value of NO_2 concentration and the error bars represent the standard deviation for the five profiles

for the altitudes between 900 and 1500 m, so the systematic error due to beam misalignment is below 10% of the magnitude of DIAL measurements in this region. At lower altitudes (< 600 m), the range-corrected signals indicated that the transmitted beams and receiver field of view did not properly overlap. At higher altitudes (≥ 2250 m), the signal is so small compared to the background value that the statistical error is larger. Differences in the DIAL1 and DIAL2 profiles may also result from differences in the laser beam receiver field of view overlaps for on-line and off-line wavelengths. However, careful beam alignment made the laser beam of on-line and off-line wavelength overlap very precisely. Even though the overlap may slightly change when the wavelength pairs are switched from DIAL1 to DIAL2, the difference is very small, and thus can be neglected. In general, the two DIAL profiles should coincide if the atmospheric conditions were the same, but Fig. 1 shows that the two DIAL profiles are slightly different, because the atmospheric conditions might have changed during the time interval between DIAL1 and DIAL2, which was 14 minutes. In Figs. 1 and 2, the height-averaged standard deviation of the five profiles for DIAL1 and DIAL2, were estimated to be $\sigma_N = 7.6$ ppb and 4.7 ppb, respectively. The statistical error for the 10 min measurement is taken as the standard deviation of the mean value, which is $\sigma_N/\sqrt{5}$, or 3.4 ppb and 2.1 ppb, respectively.

To observe the temporal change in NO_2 concentration profiles, similar measurements were performed from 13:00 on December 20,1999 to 13:00 on December 21,1999. Figure 3 shows NO_2 concentration profiles for heights 900–2250 m with 150 m range resolution, which was obtained from the average value of DIAL1 and DIAL2 for each measurement. Data for altitude below 900 m is not shown, because the null error was large. Figure 3 illustrates that NO_2 concentration varied with altitude and time. In Fig. 3 the red color means high concentration, and blue color means low concentration. At about 23:00 on December 12,1999, a peak value appeared at 1200 m, which may be due to the passage of an air mass containing high concentrations of NO_2 across the measurement region of the lidar system.

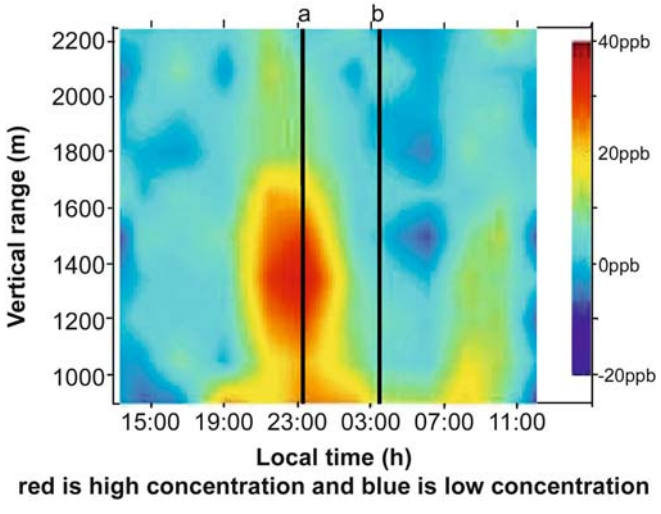

FIGURE 3 Temporal evolution of vertical NO_2 concentration profile obtained from the average of DIAL1 and DIAL2 with a 150 m the range resolution

4 Theory of error analysis

To evaluate the NO_2 measurement error, systematic errors from aerosols and beam misalignment, and statistical errors must be considered. The concentration profile can be obtained from the lidar equation

$$N(z) = \frac{1}{2\Delta\sigma}\left\{\frac{\mathrm{d}}{\mathrm{d}z}\left[-\ln\frac{p_{\lambda_{\mathrm{on}}}(z)}{p_{\lambda_{\mathrm{off}}}(z)}\right] + B + E\right\} \tag{2}$$

$$B = \frac{\mathrm{d}}{\mathrm{d}z}\left[\ln\frac{\beta_{\mathrm{on}}(z)}{\beta_{\mathrm{off}}(z)}\right] \tag{3}$$

$$E = -2\left[\alpha_{\lambda_{\mathrm{on}}}(z) - \alpha_{\lambda_{\mathrm{off}}}(z)\right]. \tag{4}$$

We can obtain the range resolved concentration profile of the target species from (1), which is same as (2) except for the two terms B and E on the right hand side. The terms B and E describe the contribution of differential backscatter and extinction by aerosols and can be calculated from (3) and (4). $\beta_{\mathrm{on}}(z)$ and $\beta_{\mathrm{off}}(z)$ in (3) represent the total atmospheric volume backscatter coefficient at range z at the "on" and "off" wavelengths. $\alpha_{\lambda_{\mathrm{on}}}$ and $\alpha_{\lambda_{\mathrm{off}}}$ in (4) denote the total extinction coefficient, excluding that of target species at range at the "on" and "off" wavelengths. From (3) and (4) we can estimate the error due to aerosols associated with the return signal or range corrected signal. The error arises from two sources: systematic error and statistic error, which are considered in detail in the following sections.

The systematic error ε_s comes from neglecting terms B and E in (2), which can be calculated with the atmospheric molecular and aerosol profiles [7],

$$\varepsilon_s = \varepsilon_{sB} + \varepsilon_{sE} \tag{5}$$

$$\begin{aligned}
\varepsilon_{sB} = \frac{B}{2\Delta\sigma} &= \frac{1}{2\Delta\sigma}\left[\frac{\lambda_{\mathrm{off}}-\lambda_{\mathrm{on}}}{\lambda_{\mathrm{off}}}\frac{\mathrm{d}}{\mathrm{d}z}\frac{(4-n)\left[R_{\lambda_{\mathrm{off}}}(z)-1\right]}{R_{\lambda_{\mathrm{off}}}(z)}\right] \\
&= \frac{1}{2\Delta\sigma}\left[\frac{\lambda_{\mathrm{off}}-\lambda_{\mathrm{on}}}{\lambda_{\mathrm{off}}}(4-n)\frac{\mathrm{d}}{\mathrm{d}z}\left(1-\frac{1}{R_{\lambda_{\mathrm{off}}}(z)}\right)\right] \\
&= \frac{1}{2\Delta\sigma}\frac{\lambda_{\mathrm{off}}-\lambda_{\mathrm{on}}}{\lambda_{\mathrm{off}}}(n-4)\frac{\mathrm{d}}{\mathrm{d}z}\left(\frac{1}{R_{\lambda_{\mathrm{off}}}(z)}\right) \\
&= \frac{1}{2\Delta\sigma}\frac{\lambda_{\mathrm{off}}-\lambda_{\mathrm{on}}}{\lambda_{\mathrm{off}}}(n-4)\frac{\mathrm{d}}{\mathrm{d}z} \\
&\quad\times\left(\frac{\beta_{\mathrm{mol,off}}(z)}{\beta_{\mathrm{mol,off}}(z)+\dfrac{P_{\mathrm{aer},\pi,\lambda}(z)}{4\pi}\alpha_{\mathrm{aer,off}}}\right) \\
&= \frac{1}{2\Delta\sigma}\frac{\lambda_{\mathrm{off}}-\lambda_{\mathrm{on}}}{\lambda_{\mathrm{off}}}(n-4)\frac{\mathrm{d}}{\mathrm{d}z}\left(\frac{1}{1+\dfrac{P_{\mathrm{aer},\pi,\lambda}(z)}{4\pi}\dfrac{\alpha_{\mathrm{aer,off}}}{\beta_{\mathrm{mol,off}}}}\right) \\
&= \frac{1}{2\Delta\sigma}\frac{\lambda_{\mathrm{off}}-\lambda_{\mathrm{on}}}{\lambda_{\mathrm{off}}}(n-4)\frac{\mathrm{d}}{\mathrm{d}z}\left(F\left(\frac{P_{\mathrm{aer},\pi,\lambda}(z)}{4\pi}\frac{\alpha_{\mathrm{aer,off}}}{\beta_{\mathrm{mol,off}}}\right)\right)
\end{aligned} \tag{6}$$

$$\varepsilon_{sE} = \frac{E}{2\Delta\sigma} = \frac{\lambda_{\mathrm{off}}-\lambda_{\mathrm{on}}}{\Delta\sigma\lambda_{\mathrm{off}}}\left(-\alpha_{\mathrm{aer,off}} + 4\alpha_{\mathrm{mol,off}}\right), \tag{7}$$

where ε_{sB} and ε_{sE} are the errors due to total backscatter and extinction, respectively, which we define as backscatter error

and extinction error. $R_\lambda(z) = \beta_\lambda(z)/\beta_{\mathrm{mol}\lambda}(z)$ is the ratio of the total backscatter coefficient to molecular backscatter coefficient, and $\alpha_{\mathrm{aer,off}}$ and $\alpha_{\mathrm{mol,off}}$ are the extinction coefficients for aerosols and air molecules, respectively. The aerosol extinction and backscatter are assumed to have a power law dependence $\alpha \sim \lambda^{-n}$ and $\beta \sim \lambda^{-n}$ with respect to wavelength [8]. The Angstrom exponent n can be vary between 0 and 2.5. Because wavelengths around 450 nm are used, Rayleigh scattering and backscattering have to be considered in the aerosol retrieval. In order to obtain the ratio $R_\lambda(z)$ at low altitude, we calculate the aerosol extinction coefficient by Fernald's solution:

$$\alpha_1(r) = -\frac{S_1}{S_2}\alpha_2(r) + \frac{X(r)\exp\left[2\left(\frac{S_1}{S_2}-1\right)\int_r^R \alpha_2(r)\mathrm{d}r\right]}{\left[\frac{X(R)}{\alpha_1(R)+\frac{S_1}{S_2}\alpha_2(R)} + 2\int_r^R X(r)\exp\left[2\left(\frac{S_1}{S_2}-1\right)\int_r^R \alpha_2(r')\mathrm{d}r'\right]\mathrm{d}r,\right]} \quad (8)$$

where α and S are the volume extinction coefficient and extinction to backscatter ratio, respectively, and suffixes 1 and 2 are quantities related to aerosols and molecules, respectively. $X(r)$ is the range-squared lidar signal, and R is the range from the lidar at which a boundary condition is assigned. The extinction coefficients at the "off" wavelength can be retrieved by (8). And the extinction coefficient at the "on" wavelength can be calculated by the aerosol wavelength power law dependence $\alpha \sim \lambda^{-n}$ and $\beta \sim \lambda^{-n}$ with respect to wavelength. Figures 4 and 5 represent the aerosol extinction coefficient at the off wavelength calculated by (8). In Fig. 4, the upper panel shows the range-corrected signal, the lower panel shows the aerosol extinction coefficient in the presence of an inhomogeneous atmosphere layer, in Fig. 5, the upper panel shows the range-corrected signal, the lower panel shows the

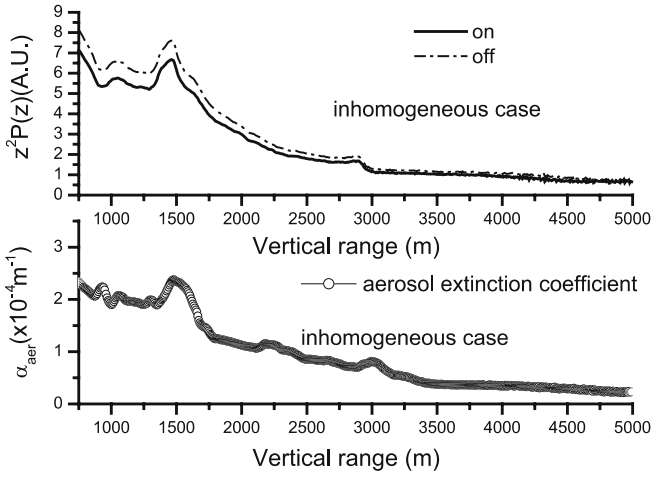

FIGURE 4 *Up panel* is the range-corrected signal, *lower panel* is aerosol extinction coefficient calculated from up panel signal at off wavelength in the presence of inhomogeneous atmosphere layer

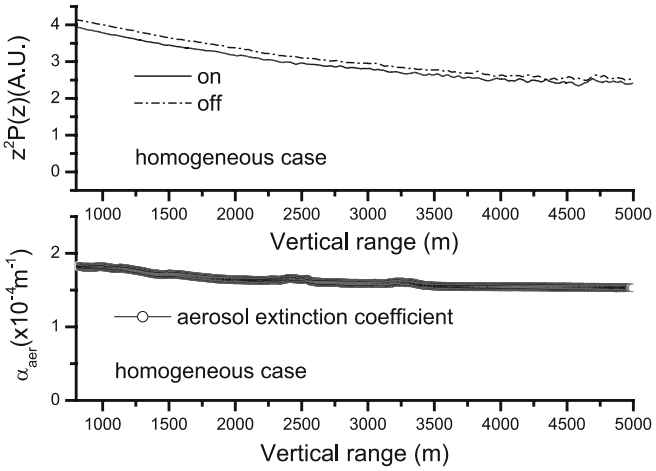

FIGURE 5 *Up panel* is the range-corrected signal, *lower panel* is aerosol extinction coefficient calculated from the up panel signal at off wavelength in a homogeneous atmosphere

aerosol extinction coefficient in the presence of homogeneous atmosphere.

The aerosol backscatter profile at the off wavelength can be obtained by (8), with the following condition:

$$\beta_{\mathrm{aer},\lambda}(z) = \frac{P_{\mathrm{aer},\pi,\lambda}(z)}{4\pi}\alpha_{\mathrm{aer},\lambda}(z). \quad (9)$$

where the inverse lidar ratio $P_{\mathrm{aer},\pi,\lambda}(z)/4\pi = 0.013\ \mathrm{sr}^{-1}$, $0.028\ \mathrm{sr}^{-1}$,$0.05\ \mathrm{sr}^{-1}$ (lidar ratio of 75 rs, 35 rs, and 20 rs) is assumed [9]. Therefore, the backscatter error can be obtained by (6). Similarly, via (7) the extinction error can also be found.

The systematic error from beam misalignment is obtained from the null profiles. In theory, if the beam profiles were identical and were precisely aligned, the value for the null profiles should be identically zero in the absence of statistical error. Therefore, the average deviation of the null profiles from zero provides a measure of how precisely the beams were aligned. Thus, we define the average deviation of null profiles from zero as the null error, and treat it as systematic error due to beam misalignment.

The statistical error was taken as the average standard deviation of five DIAL1 and DIAL2 profiles in the height range 900–2250 m.

The error due to the uncertainty of the absorption cross section of NO_2 was estimated using values from the literature [6]. Considering the temperature and pressure effects on the NO_2 absorption cross section, the uncertainty was estimated to be less than 3% over 250 nm at 294 K, 3% over 333 nm at 220 K, and less than 3% at longer wavelength. In this paper, the uncertainty of the NO_2 absorption cross section is taken to be 2.5%.

The measurement errors are due to several factors, and the total error is given by

$$\varepsilon = \sqrt{\varepsilon_{\mathrm{null}}^2 + \varepsilon_s^2 + \varepsilon_{\mathrm{sta}}^2 + \varepsilon_{\mathrm{abs}}^2} \quad (11)$$

where $\varepsilon_{\mathrm{null}}$ is the error from laser beam misalignment, ε_s is the error due to the aerosol, $\varepsilon_{\mathrm{sta}}$ is the statistical error, and $\varepsilon_{\mathrm{abs}}$ denotes the error due to uncertainty of absorption cross section.

5 Aerosol-related error

According to the (6) and (7), we can calculate the aerosol backscatter error and aerosol extinction coefficient error. By the aerosol wavelength power law dependence $\alpha \sim \lambda^{-n}$ and $\beta \sim \lambda^{-n}$, we assume the Angstrom exponent n as 0.5, 1, 1.5, and 2.0. We also assume the inverse lidar ratio as $P_{\mathrm{aer},\pi,\lambda}(z)/4\pi = 0.013\,\mathrm{sr}^{-1}, 0.028\,\mathrm{sr}^{-1}, 0.05\,\mathrm{sr}^{-1}$. We made the aerosol backscatter error calculation according to (6) at different Angstrom exponents and different lidar ratio values. Figure 6 shows the backscatter error in the presence of an inhomogeneous aerosol layer and a homogeneous atmosphere. In Fig. 6, the upper panel shows the backscatter error in the presence of an inhomogeneous layer with the assumption of $n = 0.5$ & lidar ratio $= 1/0.013$, $1/0.028$, $1/0.05$ (lidar ratio $= 75$ sr, 35 sr, 20 sr). The three profiles represent the backscatter errors with huge fluctuation at the same Angstrom exponent and different lidar ratio; the lower panel shows the backscatter error profiles in homogeneous atmosphere with the same assumptions as in the upper panel. The three profiles represent the backscatter errors at the same Angstrom exponent and different lidar ratio, the profiles show in the case of an homogeneous atmosphere that the backscatter error is very small due to the absence of large aerosol gradients. In Fig. 7, the upper panel shows the backscatter error in the presence of an inhomogeneous layer with the assumption of $n = 1.0$ and lidar ratio $= 1/0.013$, $1/0.028$, $1/0.05$; the lower panel is the backscatter error in homogeneous atmosphere with the same assumption as in the upper panel. In Fig. 8, the upper panel shows the backscatter error in the presence of an inhomogeneous layer with the assumption of $n = 1.5$ and lidar ratio $= 1/0.013$, $1/0.028$, and $1/0.05$; the lower panel shows backscatter error in homogeneous atmosphere with the same assumption as in the upper panel. In Fig. 9, the upper panel shows backscatter error in the presence of an inhomogeneous layer with the assumption of $n = 2.0$ and lidar ratio $= 1/0.013$, $1/0.028$, and $1/0.05$; the lower panel shows backscatter error in homogeneous atmosphere with the same assumption as in the up panel. In Fig. 6, 7, 8 and 9, we can see that the structures of the backscatter error profiles are quite similar at different lidar ratio values for all different Angstrom exponent values. For comparison of backscatter errors at different Angstrom exponents of n, we show an analysis in Fig. 10. In Fig. 10, the upper panel shows backscatter error in the presence of an inhomogeneous layer with the assumption of lidar ratio $= 1/0.05$ and $n = 0.5$, 1.0, 1.5, 2.0; the lower panel shows backscatter error in homogeneous atmosphere with the same assumption as in the upper panel. From Fig. 10, we can see that in case of the same lidar ratio, the backscatter error is proportional to the Angstrom exponent of n, the larger the backscatter error the larger the Angstrom exponent of n. Equation (6) coincides with this. It is easy to see the difference in the inhomoge-

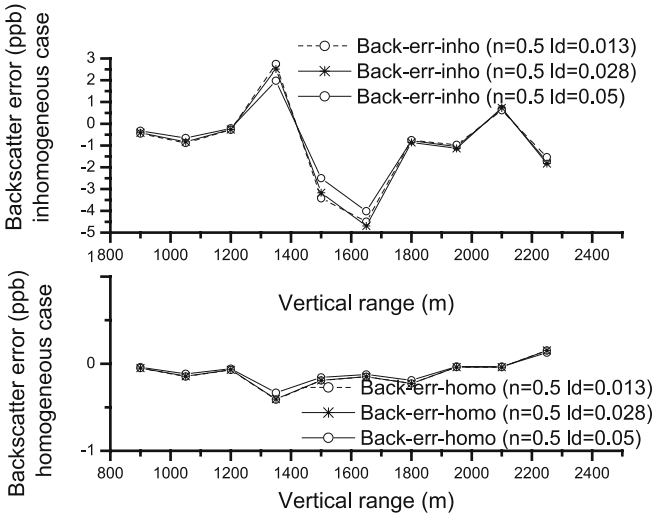

FIGURE 6 *Up panel* shows the backscatter errors in the present of an inhomogeneous layer with the assumption of $n = 0.5$ and lidar ratio $= 1/0.013$, $1/0.028$, $1/0.05$; *lower panel* shows the backscatter errors in homogeneous atmosphere with the same assumption as in the *up panel*

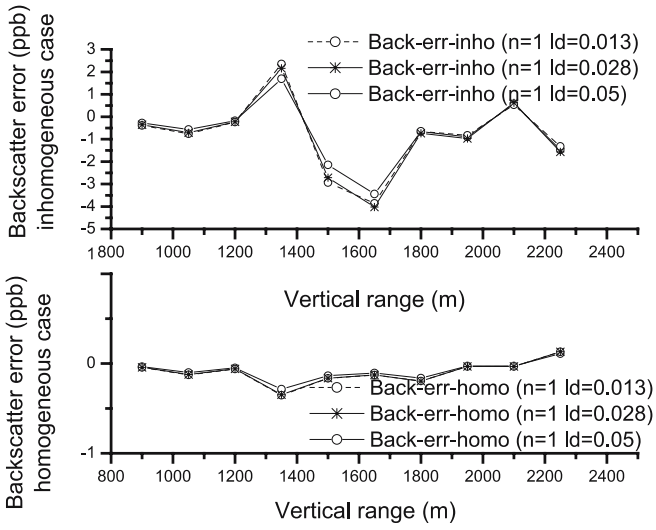

FIGURE 7 *Up panel* shows the backscatter errors in the present of an inhomogeneous layer with the assumption of $n = 1.0$ and lidar ratio $= 1/0.013$, $1/0.028$, $1/0.05$; *lower panel* shows the backscatter errors in homogeneous atmosphere with the same assumption as in the *up panel*

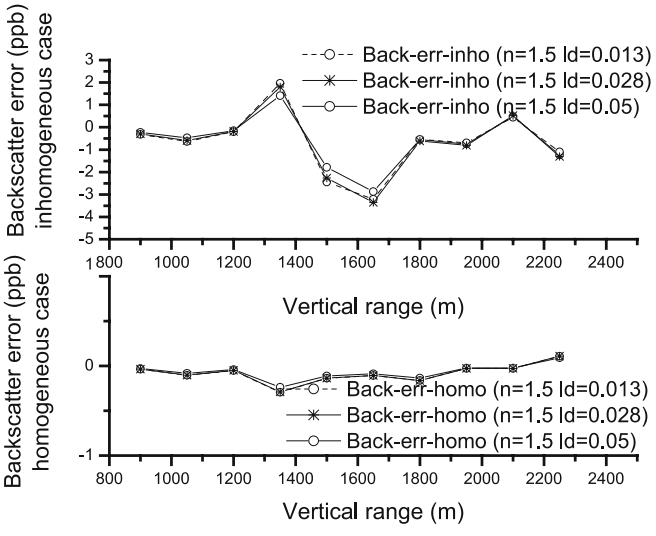

FIGURE 8 *Up panel* shows the backscatter errors in the present of an inhomogeneous layer with the assumption of $n = 1.5$ and lidar ratio $= 1/0.013$, $1/0.028$, $1/0.05$; *lower panel* shows the backscatter errors in homogeneous atmosphere with the same assumption as in the *up panel*

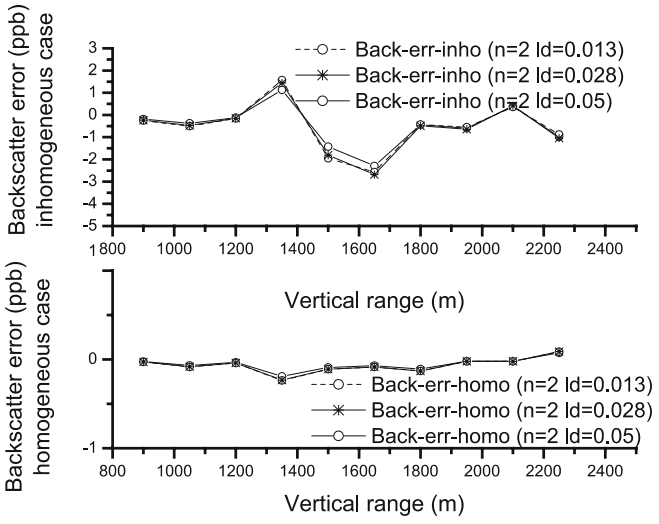

FIGURE 9 *Up panel* shows the backscatter errors in the present of an inhomogeneous layer with the assumption of $n = 2.0$ and lidar ratio $= 1/0.013$, $1/0.028$, $1/0.05$; *lower panel* shows the backscatter errors in homogeneous atmosphere with the same assumption as in the *up panel*

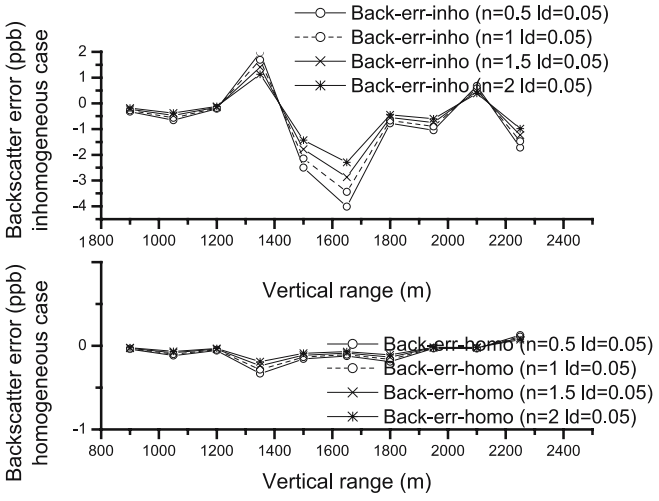

FIGURE 10 *Up panel* shows the backscatter errors in the present of an inhomogeneous layer with the assumption of $n = 0.5$, 1.0, 1.5, 2.0 and lidar ratio $= 1/0.05$; *lower panel* shows the backscatter errors in homogeneous atmosphere with the same assumption as in the *up panel*

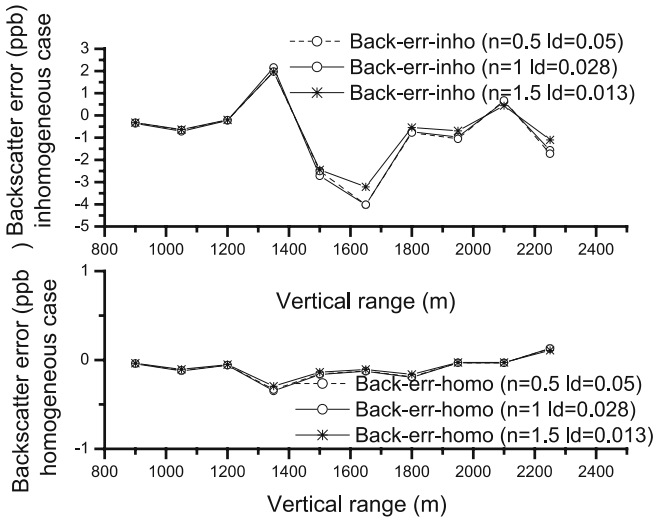

FIGURE 11 *Up panel* shows the backscatter errors in the present of an inhomogeneous layer with the assumption of $n = 0.5$ & lidar ratio $= 1/0.05$ and $n = 1.0$ & lidar ratio $= 0.028$ and $n = 1.5$ & lidar ratio $= 1/0.013$; *lower panel* shows the backscatter errors in homogeneous atmosphere with the same assumption as in the *up panel*

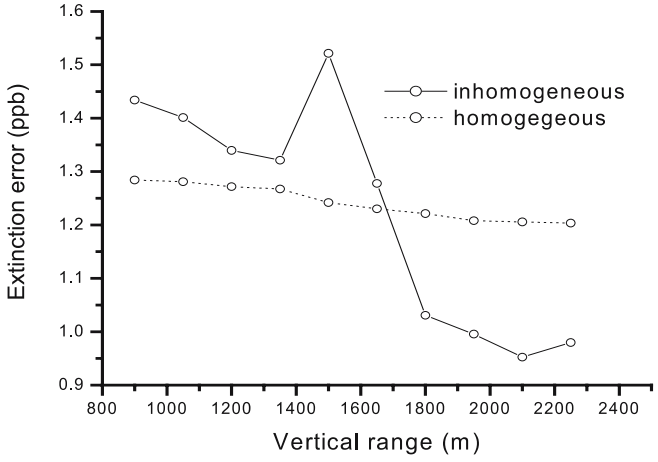

FIGURE 12 The *solid line* is the extinction error in the present of an inhomogeneous layer; and the *dash line* is the extinction error in homogeneous atmosphere for any aerosol optical property assumptions

neous case. However, in the homogeneous case, all profiles are compressed together except for the point at $z = 1350$ m. This is because the values of backscatter error are very small in the case of homogeneous atmosphere in general. We compare backscatter errors for some special cases in Fig. 11. The upper panel presents the three backscatter error profiles in the presence of an inhomogeneous layer with the assumption of $n = 0.5$ & lidar ratio $= 1/0.05$ and $n = 1.0$ & lidar ratio $= 1/0.028$ and $n = 1.5$ & lidar ratio $= 1/0.013$, respectively. The lower panel presents the three backscatter error profiles in homogeneous atmosphere with the same assumption as in the upper panel. From Fig. 11, we can see that in inhomogeneous atmosphere conditions the backscatter error profiles in the cases of $n = 0.5$ & lidar ratio $= 1/0.05$ and $n = 1.5$ & lidar ratio $= 1/0.013$ are slightly different from the case of $n = 1$ & lidar ratio $= 1/0.028$. It demonstrates that the value of backscatter error is also affected by the function of the lidar ratio. According to (6), the value of backscatter error is proportional to the gradient of $\frac{1}{R_{\lambda_{\text{off}}}(z)}$. The gradients vary a lot at different locations (height). In comparison within Fig. 6, 7, 8, 9, 10 and 11, the contribution of n to values of backscatter errors is larger than the lidar ratio. In other words, the value of backscatter error is more sensitive to the Angstrom exponent of n than the lidar ratio. According to (7), the aerosol extinction error does not depend on the Anstronent exponent of n and lidar ratio. In other words, for any aerosol optical property assumptions the aerosol extinction coefficient error is the same. Figure 12 shows the aerosol extinction error. The solid line is the extinction error in the presence of an inhomogeneous layer; and the dash line is extinction error in homogeneous atmosphere. In order to check what happens for the resulting NO_2 profiles in different cases with different aerosol optical property assumptions, we com-

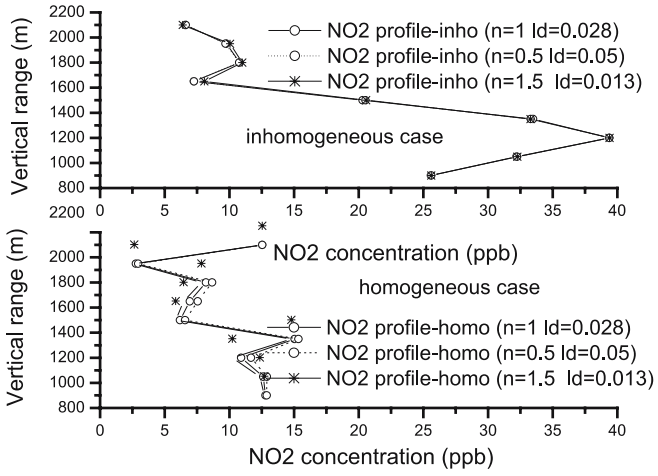

FIGURE 13 *Up panel* is the NO_2 concentration profiles of the average of DIAL1 and DIAL2 in an inhomogeneous atmosphere with the aerosol corrections with the three different assumptions of $n = 1$ & lidar ratio $= 1/0.028$ and n=0.5 & lidar ratio $= 1/0.05$ and $n = 1.5$ & lidar ratio $= 1/0.013$; *lower panel* is the NO_2 concentration profiles of the average of DIAL1 and DIAL2 in homogeneous atmosphere with the aerosol corrections with the same assumptions as in the *up panel*

pare cases for when with Angstrom values of of 0.5 and 1.5 and a lidar ratio of $1/0.05$ and $1/0.013$ are assumed, and with an extreme case with a simple Angstrom value of 1 and a lidar ratio of $1/0.028$ is assumed. We do aerosol backscatter and extinction corrections to NO_2 profiles in the above three different cases, and it is shown in Fig. 13. The upper panel shows the NO_2 profiles of the mean value of DIAL1 and DIAL2 with three different aerosol corrections in the presence of an inhomogeneous aerosol layer. Variation of about 1 ppb presents at a height of 1650 m between the case with an Angstrom of 1.5 and lidar ratio of $1/0.013$ assumed, and the case of an Angstrom of 1 and lidar ratio of $1/0.028$ assumed. The variation of NO_2 concentration due to different aerosol optical property assumptions is changeable at different heights. The variation of NO_2 concentration is less than 1 ppb at a height of 1800 m, 1950 m, 2100 m and 2250 m. In the homogeneous case, the variations are much smaller than the inhomogeneous case, and can not be shown clearly in the lower panel in Fig. 13.

6 Total error estimation of measured data

The measurement errors for obtained data were estimated according to the discussion in the above section. As an example, Figs. 4 and 5 represent two typical sets of data obtained from an inhomogeneous atmosphere and a clear atmosphere (homogeneous atmosphere), respectively. The upper panel of Fig. 4 is the range corrected signal in the case of an inhomogeneous atmosphere, obtained at around 23:00 on Dec.20, 1999. The signal is not smooth owing to aerosols at altitude 900–1800 m. In comparison, the range corrected signal in the case of a clear atmosphere, which was obtained at around 3:00 on Dec.21, 1999, is shown in the upper panel of Fig. 5. In this case, the signal was smoother, indicating the absence of large aerosol gradients. The lower panel of Figs. 4 and 5 shows the extinction coefficients calculated by (8). Figure 4 shows that the extinction coefficient in the presence

Source of error	Measurement error (ppb)	
	Inhomogeneous atmosphere	Clear atmosphere
Systematic error from aerosols (ε_s)	< 4.44 (peak value at the assumption of $n = 0.5$ and lidar ratio $= 1/0.013$).	< 1.49 (peak value at the assumption of $n = 0.5$ and lidar ratio $= 1/0.013$).
Null error (ε_{null})	< 2	< 2
Mean statistical error (ε_{std})	3.4	2.1
Absorption cross section error (ε_{abs})	< 1.1	< 1.1
Total error	< 6.0	3.4

TABLE 1 Measurement errors of NO_2 in the presence of an inhomogeneous atmospheric layer and in the case of a clear atmosphere. The null error is the average value over the observation interval of 24 hours

of additional inhomogeneous atmospheric layers vary with a large fluctuation, while Fig. 5 shows that the aerosol extinction gradient is small in a clear atmosphere. The aerosol error was estimated via (5)–(7) as discussed in the section "Theory of error analysis". In comparison of Fig. 6, 7, 8, 9 and 10, the peak values of backscatter error are present in Fig. 6, being about $+2.9$ and -4.9 ppb in the case of inhomogeneous atmosphere and $+0.2$ and -0.4 ppb in the case of homogeneous atmosphere with the assumption of $n = 0.5$ and lidar ratio=$1/0.013$. Figure 12 is the extinction error with peak values of $+1.54$ ppb in the inhomogeneous case and $+1.29$ ppb in the homogeneous case. The total aerosol error is the sum of Figs. 6 and 12, with a peak value of 4.44 ppb ($|2.9 + 1.54|$) $|-4.9 + 1.54|$) in the inhomogeneous case and 1.49 ppb ($|0.2 + 1.29|$) $|-0.4 + 1.29|$) in the homogeneous case. In the case of a clear atmosphere, the error due to aerosols did not vary much with altitude, and the error was much lower than in the inhomogeneous case. Large systematic errors due to aerosols occur when an aerosol gradient is present.

The error due to uncertainty of absorption cross section was estimated to be at most 1.1 ppb. The null error was obtained as the average value of the null profile from 13:00 on Dec.20,1999 to 13:00 on Dec.21,1999. The measurement errors are summarized in Table 1.

7 Summary

This paper presented DIAL measurement of NO_2 vertical concentration profiles and an estimation of the measurement errors. The obtained NO_2 concentration was 0–40 ppb, and varied with time and altitude. We mainly paid attention to error estimation including systematic error from aerosol and laser beam misalignment. Aerosol error was < 4.44 ppb in the presence of inhomogeneous atmospheric layers and < 1.49 ppb in the case of a clear atmosphere with the assumption of $n = 0.5$ and lidar ratio $= 1/0.013$. The average systematic error from beam misalignment, which was obtained from the null profiles, was < 2 ppb. Considering the systematic error, statistical error and absorption cross-section error, the total error is 6.0 ppb in the presence of an inhomogeneous atmospheric layer and < 3.4 ppb in the case of a clear atmosphere.

ACKNOWLEDGEMENTS Parts of the study are supported by the nature science research plan of university in Jiangsu province of China under contract 05KJB170073.

REFERENCES

1 B.J. Finlayson-Pitts, *Atmospheric Chemistry* (1948) pp 406–425
2 K.A. Fredriksson, H.M. Hertz, Appl. Opt. **23**, 1403 (1984)
3 Z. Wang, J. Zhou, H. Hu, Z. Gong, Appl. Phys. B **62**, 143 (1996)
4 V.A. Kovalev, J.L. McElroy, Appl. Opt. **33**, 8393 (1994)
5 Z. Wang, H. Hu, J. Zhou, "Dual-DIAL measurements of ozone profiles", in 17th Int. Laser Conf., Abstracts of Papers (Sendai Int. Center, Sendai, Japan, 1994), pp. 54–57
6 A.C. Vandaele, C. Hermans, P.C. Simon, M. Carleer, R. Coln, S. Fally, M.F. Merienne, A. Jenouvrier, B. Coquart, J. Quant. Spectrosc. Radiant. Transfer **59**, 171 (1998)
7 Z. Wang, H. Nakane, H. Hu, J. Zhou, Appl. Opt. **36**, 1245 (1997)
8 F. Fernald, Appl. Opt. **23**, 652 (1984)
9 E.V. Browell, S. Ismail, S.T. Shipley, Appl. Opt. **24**, 2827 (1985)